Dry reforming of methane to test passivation stability of Ni/ Al_2O_3 catalysts

Franz, Robert; Tichelaar, Frans D.; Uslamin, Evgeny A.; Pidko, Evgeny A.

DOI
10.1016/j.apcata.2021.117987

Publication date
2021

Document Version
Final published version

Published in
Applied Catalysis A: General

Applied Catalysis A, General 612 (2021) 117987

Contents lists available at ScienceDirect

Applied Catalysis A, General

journal homepage: www.elsevier.com/locate/apcata

Dry reforming of methane to test passivation stability of Ni/ Al_2O_3 catalysts

Robert Franz [a], Frans D. Tichelaar [b], Evgeny A. Uslamin [a,c], Evgeny A. Pidko [a,*]

[a] Inorganic Systems Engineering Group, Chemical Engineering Department, Delft University of Technology, Van der Maasweg 9, 2629 HZ, Delft, the Netherlands
[b] Kavli Institute of Nanoscience, Delft University of Technology, Lorentzweg 1, 2628 CJ, Delft, the Netherlands
[c] TsyfroCatLab Group, University of Tyumen, Volodarskogo St.6, 625003, Tyumen, Russia

ARTICLE INFO

Keywords:
Heterogeneous catalysis
Dry reforming of methane
Passivation
Nickel
Catalyst deactivation

ABSTRACT

Catalyst passivation refers to the formation of a protective oxide layer on the active metal particles that prevents their oxidation when exposed to air. Common passivation procedures, when applied to Ni/ Al_2O_3 catalysts, typically result in a significant decrease of the overall Ni surface area and, accordingly, the catalytic activity. Nevertheless, passivation and reactivation is an attractive pre-treatment option for this system. Ni/ Al_2O_3 typically requires reduction temperatures much higher than the desired reaction temperature, whereas reactivation of passivated samples is a low-temperature reduction. This can be used to avoid temperature limitations of existing systems. Thus, more insight into the passivation process of this system is desirable. In this work we analyzed the impact of passivation on the catalytic performance of a series of Ni/ Al_2O_3 catalysts in dry reforming of methane. This approach allows for the elimination of scale effects during passivation. We show that changes in conversion and especially of the coke content can be used to track sintering of Ni particles. These metrics allows to identify an adverse effects of catalyst passivation in excess O2, which gives rise to rapid local overheating and, accordingly, Ni sintering even when operating at tens of mg catalyst scale. Our study demonstrates that such problems are not limited to scaling issues and sufficient care must be taken even on a lab-scale when passivating Ni/ Al_2O_3 catalysts.

1. Introduction

Supported nickel catalysts are a common subset of heterogeneous catalysts for various industrial applications. Both the high inherent catalytic activity of nickel as well as the abundance make it an attractive active metal. Consequently, nickel-based catalysts have been investigated and employed for such reactions as methane/ hydrocarbon reforming [1–3], CO_2 methanation [4–8] and other hydrogenation reactions [9–13]. In hydrogenation and reforming reactions, the catalytically active substance is metallic nickel, requiring a dedicated reduction step. The most straightforward solution would be to activate the catalyst in the reactor system by reducing it directly prior to the catalytic process. However, such a one-pot activation-reaction scheme may be hampered or even prohibited by the large temperature gap between the two procedures.

While many catalysts can be reduced at moderate temperatures (200–600 °C) [14,15], Ni supported on such materials as Al_2O_3 or $MgAl_2O_4$ can require temperatures of 800 °C or higher, to achieve full reduction of the active phase [16–19]. Most hydrogenation reactions such as CO_2 or alkene hydrogenation proceed at temperatures well below 500 °C. A reactor suitable for high temperatures only for in-place reduction would not be cost-effective, especially on an industrial scale. Instead, a passivated catalyst can be used [20]. In this approach the catalyst is first activated in a dedicated setup via a hightemperature reduction, followed by cooling the activated catalyst and exposing it to low levels of oxidant. This treatment enables the formation of a protective superficial layer of metal oxide on the reduced metal particles. The surface oxide layer acts as a barrier for deep bulk oxidation of surface nanoparticles allowing thus for safe transport to the catalytic reactor. The reduction of this surface oxide layer can be accomplished under milder conditions than the bulk oxide reduction and therefore can be carried out directly in the catalytic reactor prior to the reaction or in situ [21]. On an industrial scale, a shorter reduction period also reduces the downtime before production can be continued [20].

Catalyst passivation approach is particularly useful for the cost-effective design of reactors. This is well reflected in the many patents incorporating catalyst passivation techniques [22–24]. Many academic studies have been devoted to this topic as well [21,25–32]. Ni catalysts using either SiO_2 or Al_2O_3 supports are two of the most popular model systems [25–27,29–31]. For Ni/ SiO_2 the general conclusion in literature

* Corresponding author.
E-mail address: e.a.pidko@tudelft.nl (E.A. Pidko).

https://doi.org/10.1016/j.apcata.2021.117987
Received 18 August 2020; Received in revised form 26 December 2020; Accepted 30 December 2020
Available online 4 January 2021

is, that passivation treatments allows for full recovery of the metal surface area with marginal effects on the particle size distribution. [26, 30] At the same time, the moderate reduction temperature of typical Ni/ SiO_2 catalysts (usually less than 500 °C [33]) limit the necessity of such a protocol in the first place.

In the case of the Al_2O_3-supported catalysts, the situation is much more complex. While some authors mention a loss in metal surface area as a result of passivation and reactivation [26,27], a preservation of total nickel surface area has also been reported [25]. Unfortunately, the only procedural detail mentioned for the latter was the oxygen concentration of 0.2 %. Information on the sample mass is critical, because of the scale-dependency of potential heat effects and the associated structural changes during the passivation [25].

Heat management during the passivation procedure critically depends on the scale of the operation. Scaling effects will certainly play an important role in an industrial setting, but on a lab-scale the situation is less clear. Exothermic reactions at low temperatures (such as CO oxidation [34,35]) have been noted to lead to overheating of catalytically active metallic particles on metal oxide supports. If such local overheating effects can cause substantial structural modifications of the supported catalysts, the passivation of small amounts of sample can already become challenging. The higher reduction temperatures of Ni/ Al_2O_3 compared to Ni/ SiO_2 make the passivation particularly attractive for the former. Thus, further understanding of the process would be of help for the design and optimization of practical passivation procedures.

In the above-mentioned literature examples H_2 chemisorption is the method of choice to quantify the impact of passivation but this requires sample sizes of more than 100 mg. To reduce the catalyst amounts during passivation and thus eliminate scaling effects as far as possible, we chose dry reforming of methane as a probe reaction. Dry reforming of methane refers to the high-temperature conversion of methane and carbon dioxide to syngas ($CO+H_2$):

$$CH_4 + CO_2 \longrightarrow 2CO + 2H_2 \; \Delta H_{298K} = 247 \text{ kJ mol}^{-1} \quad (1)$$

Several considerations have led to an active interest in dry reforming research in recent years. Firstly, large scale reduction of CO_2 emission are desirable to contain the effects of global warming [36]. Incorporating CO_2 into methane reforming represents a relatively moderate modification of a single process step in the chemical supply chain. Secondly, the use CO_2 as a feedstock in methane reforming provides syngas with a higher CO to H_2 ratio that can be desirable for the syntheses of bulk chemicals such as acetic acid [37].

In this work we systematically investigate the impact of passivation and reactivation on Ni/ Al_2O_3-catalysts. The samples were prepared through conventional incipient wetness impregnation and thoroughly characterized. We were able to show how Ni loading affects the reducibility and surface area of Ni through a combination of TEM, N_2O titration, TPR and N_2 physisorption. The effects on the catalytic performance were evaluated using dry reforming of methane as a probe reaction. Dry reforming is a suitable probe reaction to investigate the effects of passivation and activation on the catalytic properties for several reasons. Firstly, 10 mg of catalyst are sufficient to achieve significant levels of conversion over extended periods of time [38]. Thus, this approach allows us to reduce, passivate and analyze on a scale of less than 30 mg, eliminating heat effects from neighboring catalyst particles as much as possible. Secondly, the elevated carbon levels compared to pure steam reforming lead to a higher susceptibility for coking [39].

Coke nuclei form preferentially at step-edge sites and on large facets of the Ni surface [1,40]. Small terrace sites on the other hand do not allow for the formation of stable nuclei. Consequently, changes in conversion and different coke contents after dry reforming should allow the direct probing of the effects of catalyst passivation. Mild overheating with moderate sintering would yield slightly larger particles that produce more coke. Significant overheating and sintering on the other hand would give rise to a noticeable decrease in Ni surface area and thus of coke content and conversion as well.

Our analysis reveals that the oxygen concentration used during passivation has a pronounced effects on Ni dispersion. Non-ideal passivation parameters are reached very quickly and negatively affect the performance almost independently of the amount of catalyst mass used.

2. Experimental

2.1. Chemicals

Ethylenediaminetetraacetic acid (EDTA, ThermoFisher 99 %), NH_3 solution (VWR, 25 %), SAS90 Al_2O_3 catalyst support (BASF Nederland B. V.), $Ni(NO_3)_2 \cdot 6H_2O$ (Merck, analysis quality). All materials were used as received except for NH_3 (aq), which was diluted with demineralized water in a volumetric ratio of 1:1 before usage, and SAS90. The SAS90 Al_2O_3 spheres were ground to a fine powder (< 212 μm) before impregnation.

2.2. Catalyst preparation

All samples were synthesized via incipient wetness impregnation. In a typical synthesis, EDTA and $Ni(NO_3)_2$ with a Ni^{2+}/ EDTA molar ratio of 1 were dissolved in aqueous 12.5 % ammonia solution. This solution is then immediately used for impregnation. Per impregnation step an amount of $Ni(NO_3)_2$ was used to increase the loading of Ni on the support by 0.04 $g_{Ni}\, g_{support}^{-1}$. After impregnation, the solid was dried at 80 °C for 5 h and calcined at 700 °C for 5 h (heating rate of 10 K min^{-1}). For the samples with a loading of more than 0.04 g g^{-1} this procedure of impregnation, drying and calcination was repeated as often as necessary. In total, four different loadings were synthesized: 0.04, 0.08, 0.12 and 0.24 g g^{-1}. All batches were synthesized in duplicate. ICP-OES was used to determine the final Ni loading.

2.3. Catalyst characterization

Temperature programmed reduction (TPR) was carried out in a dedicated setup equipped with thermal conductivity detector (TCD) and mass-spectrometer (MS). For TPR measurements, 100 mg of sample (particle size 212−355 μm) were filled into a quartz reactor (I.D. of 6 mm) and the reactor placed into the furnace. Afterwards, a flow of 30 mL min^{-1} (10 % H_2 in Ar) was started. The setup was heated to 950 °C with a ramp of 10 K min^{-1}. H_2 consumption was monitored with the TCD downstream of the reactor.

Total metal Ni surface was quantified by N_2O titration using the TPR setup described above. Per experiment 200 mg of sample (particle size 212–355 μm) were mixed with 300 mg SiC (particle size 212–355 μm) and filled in a reactor quartz reactor (I.D. of 6 mm) and the reactor placed into the furnace. In a first step, the sample was reduced using a flow of 30 mL min^{-1} at 800 °C for 1 h (heating rate of 10 K min^{-1}). Then, the sample was cooled in 27 mL min^{-1} of pure Ar to 75 °C. At this temperature, a mixture of 20 % N_2O in Ar was pulsed into the reactor. This was achieved with the help of a switching valve equipped with a 100 μL loop upstream of the reactor. The N_2O and N_2 signals were tracked using mass spectrometry. N_2O was pulsed into the system until no more N_2O consumption could be detected. The Ni surface area was calculated according to the method described by *Tada et.al.* [41]

$$S_{Ni,\,cat} = \frac{n_{N2O} * N_A}{A * m_{cat}} \quad (2)$$

$$S_{Ni,Ni} = \frac{n_{N2O} * N_A}{A * m_{Ni}} \quad (3)$$

where A is the number of Ni atoms per unit area ($1.54 * 10^{19}$ m^{-2}), n_{N2O} the molar N_2O consumption as measured with mass spectrometry, N_A

Avogadro's constant and m_X the mass of either the catalyst or the reduced Ni on the catalyst. The latter was determined by integrating the TCD signal during the initial period of Ni reduction.

N_2 physisorption was carried out after drying all samples overnight at 150 °C under N_2 flow. Afterwards, the samples were loaded into a *micromeritics TriStar II*. The measurements proceeded at 77 K.

The chemical composition of the samples with regards to the Al and Ni content was determined via ICP-OES. Each sample was digested by dispersing 30 mg of solid in a mixture of 4.5 mL HCl and 1.5 65 % HNO_3 using a microwave. The microwave was set at 1000 W for 60 min. After digestion, each sample was diluted with 50 mL of MQ and analyzed with an ICP-OES 5300 DV.

TEM images were obtained using a FEI Tecnai TF20UT/STEM. The instrument was operated in STEM mode and in brightfield mode. Sample preparation before STEM-analysis consisted of a reduction of 30 mg at 800 °C in a flow of 10 % H_2 in inert followed by passivation at room temperature. Two different procedures were used for the latter: The milder procedure was carried out in a reactor tube with a reactor tube with an inner diameter of 1.5 cm. The O_2 concentration was increased every 20 min to the following levels: 0.2 %, 1%, 3%, 10 % and 20 %. The harsher procedure was carried out in the same setup as the TPR measurements with steps of 3 %, 10 % and 20 %.

2.4. Catalytic testing

Samples were tested for their catalytic activity in dry reforming of methane in a single-reactor system. In this system, a quartz reactor (I.D. of 4 mm) is placed in a furnace. Upstream of the reactor, mass flow controllers (Bronkhorst) regulate the flow of N_2, CH_4, CO_2 and H_2 to the reactor. Downstream of the reactor a compact GC equipped with a TCD was used for the online product analysis. Product separation was achieved using a micropacked column (ShinCarbon ST 80/100 2 m, 0.53 mm I.D.). Conversion of methane and CO_2 was calculated using N_2 as the internal standard according to the following equation:

$$X_R = \frac{\left(A_R/A_{N2}\right)_0 - \left(A_R/A_{N2}\right)}{\left(A_R/A_{N2}\right)_0} \quad (4)$$

Where R is the reactant in question (either CH_4 or CO_2) and A is the peak area in the GC. In a typical catalytic experiment, 10 mg of sample (355–425 μm) were diluted in 140 mg of SiC (212–300 μm). This mixture was filled into the quartz reactor between two plugs of quartz wool and upstream of a 9 cm layer of SiC (212-425 μm). Upstream of the catalyst-SiC mixture, 7 cm of SiC (212425 μm) provided pre-warming of the feed. For freshly calcined samples, the sample was heated in a stream of 10 % H_2 in N_2 (50 mL min^{-1}) to 800 °C (10 K min^{-1}) and reduced at this temperature for 1 h, before being cooled to 650 °C. At this point, the flow was switched to 100 mL min^{-1} of 25 % CH_4 and 25 % CO_2 in N_2. Afterwards, dry reforming experiments were carried out for 12 h. If the sample was already pre-reduced and passivated, the sample was directly heated to 650 °C in 10 % H_2 in N_2 (50 mL min^{-1}). Once the reaction temperature was reached, the dry reforming experiment started. After each catalytic experiment, the coke content of the sample was analyzed via TGA (Mettler-Toledo TGA/SDTA 851^e). The catalytic activity of the freshly calcined sample was measured for two different batches of the same loading. The difference in catalytic activity was used to determine the experimental error. This allows for more accurate classification of the effects of passivation.

Pre-reduction and passivation were carried out in the same setup as used for the TPR and N_2O experiments. Here 25 mg of sample (355−425 μm) were used per run. The samples were reduced in 10 % of H_2 in N_2 (30 mL min^{-1}) at 800 °C for 1 h (10 K min^{-1}) and then cooled to room temperature. An ensuing passivation procedure consisted of flowing 30 mL min^{-1} of Ar-O_2 mixtures over the catalyst. Each concentration of O_2 was maintained for 20 min. The concentrations of O_2 were either 1 %, 3 %, 10 % and 20 % or 3 %, 10 % and 20 %. Alternatively, the passivation procedure could also be omitted and the freshly reduced sample was directly exposed to air.

3. Results and discussion

3.1. Catalyst characterization

To evaluate the effect of Ni loading on the physico-chemical properties of the synthesized materials, the samples were thoroughly characterized. The catalysts characterization data are summarized in Table 1. ICP data shows that the metal content in the resulting samples corresponds well with the desired incipient wetness impregnation loading. This indicates that no Ni loss occurs during the consecutive calcination steps. The textural properties of the catalysts were characterized with N_2 physisorption. The isotherms presented in Fig. S1 show similar behavior featuring adsorption on the surface. The adsorptive properties of alumina are not affected even by multiple calcination cycles (Fig. S1). However, a slight decline in BET surface area is observed for the Ni/ Al_2O_3 samples. This can be attributed to the formation of various Ni species on the surface of alumina.

TPR experiments were carried out to study the dispersion and properties of the supported Ni species. The TPR data shown in Fig. 1 indicate the presence of two features for all Ni/ Al_2O_3 samples with maxima around 850 °C and 550 °C. The high-temperature peak significantly dominates the TPR profiles for all catalysts. Increasing the loading of Ni does not affect the position of either peak, indicating a constant reduction temperature. However, an increase in Ni loading from 0.04 to 0.12 g g^{-1} leads to a significant increase in the intensity of the high temperature peak. A further increase in Ni loading to 0.24 g g^{-1} does not lead to a further increase in peak intensity. In contrast, the TPR profile of the sample with 0.24 g g^{-1} shows significantly higher reduction activity in the lower temperature range.

While the high temperature peak (850 °C) can be attributed to highly dispersed Ni particles, the low temperature reduction observed for higher Ni loadings is typically related to the bulk Ni phase [42–44]. Indeed, with increasing quantities of bulk Ni, one would expect the Ni dispersion to decrease as well. However, the results of N_2O titration experiments reveal a rather different trend. While the overall Ni surface area increases with higher loadings (Table 1), the surface area per mass of Ni and thus the dispersion does not decrease monotonously. As can be seen from the results in Fig. 2, the highest dispersion is indeed achieved at a Ni loading of 0.04 g g^{-1} and increasing the loading to 0.08 g g^{-1} does decrease the dispersion. However, a further increase in Ni content to 0.12 g g^{-1} does not affect the dispersion noticeably, while at even higher loadings, the average Ni dispersion increases again.

At the same time, increasing the Ni loading reduces the BET area continuously from 86 m^2 g^{-1} for 0.04 g g^{-1} to 62 m^2 g^{-1} for 0.24 g g^{-1}. Such a linear decrease in surface area with increasing Ni loading suggests that Ni particles are deposited on the external surface. The observed non-linearity of the Ni surface area per Ni mass can be attributed to several different factors. Firstly, the titration with N_2O is an exothermic reaction. Especially, for a Ni loading of 0.24 g g^{-1} small temperature increases were observed during the initial pulses. It stands to reason that the local temperature around the titrated surface will have

Table 1
Ni/ Al_2O_3 characterization data.

Nominal loading [g g^{-1}]	Ni loading (ICP) [g g^{-1}]	Ni area [m^2 g_{cat}^{-1}]	Ni area [m^2 g_{Ni}^{-1}]	BET surface area [m^2 g_{cat}^{-1}]
0.04	0.035	0.8	23.9	86
0.08	0.07	1.1	16.4	80
0.12	0.106	1.6	16.8	78
0.24	0.21	3.8	22.9	62

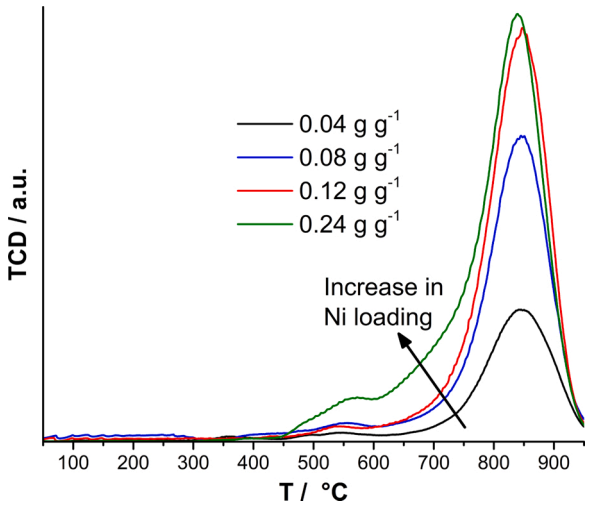

Fig. 1. Temperature-programmed reduction of the as-prepared Ni/ Al_2O_3 samples.

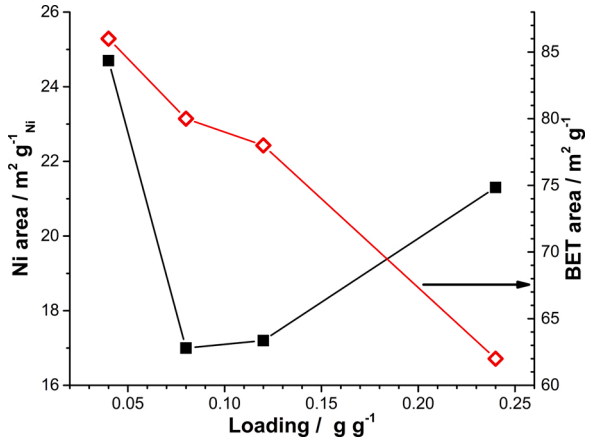

Fig. 2. BET surface area and Ni dispersion obtained from N_2O titration (in m^2 g^{-1}_{Ni}) for Ni/ Al_2O_3 catalyst samples.

increased more than the overall bed temperature. Higher temperatures are known to lead to bulk oxidation in addition to surface titration [41]. The total Ni surface increases disproportionately, when the loading is increased from 0.12 g g^{-1} to 0.24 g g^{-1} (see Table 1 and Fig. S2). A certain percentage of this increase will be due to bulk oxidation contributing to the measured N_2O consumption.

Secondly, bimodal size distributions of metal particles on catalyst supports has frequently been reported in literature [45–48]. Therefore, the development of a bimodal particle distribution could also contribute to the observed trend: At first the Ni particles are small and highly dispersed. A higher loading initially leads mainly to an increase of the average size. Adding more Ni to the support again causes the generation of smaller particles, which increases the average dispersion again.

To further elucidate the structure of the Ni on the surface, STEM-EDX measurements were carried out. To mimic the conditions before N_2O titration as best as possible, the samples underwent the same reduction procedure and were then passivated starting with an oxygen concentration of 0.2 %, as described in the experimental section. At the same time, this opportunity was used to gauge the impact of passivation by also analyzing samples that were passivated with an initial concentration of 3 % O_2. The measured particle size distributions are shown in Fig. 3.

Firstly, it must be noted, that the statistical uncertainty of these distributions cannot be neglected, because around 200 particles were measured for each sample. The observed distributions should be considered more as an indication. Nevertheless, the results of these measurements support the interpretation of the results of the N_2O titration. It can be observed, that for an initial O_2 concentration of 0.02 % an increase in Ni loading from 0.04 to 0.08 g g^{-1} leads to a significantly broader size distribution. Indeed, this is the only mildly treated sample with a considerable portion of particles of around 20 nm. For higher Ni loadings, the size distribution becomes more narrow and defined again.

When comparing the results for different initial O_2 concentrations, the higher loadings are more of interest, however. The samples with Ni loadings of 0.12 and 0.24 g g^{-1} are the those, where an increase in the average Ni size is implied for higher initial O_2 concentrations during passivation. For the other two samples, no significant impact of the initial O_2 concentration was observed. Thus, noticeable sintering appears to be particularly problematic at elevated Ni loadings.

3.2. Dry reforming of methane

Catalytic tests were carried out at a temperature of 650 °C. At this temperature coke formation is thermodynamically favored. This operating regime allows for a quicker identification of subtle differences in the morphology of the Ni surface between the different samples. In a first step, all four catalysts were tested in the standard procedure where the reduction takes place immediately prior to the catalytic run in the same reactor.

For these “baseline” measurements the conversion of methane as a

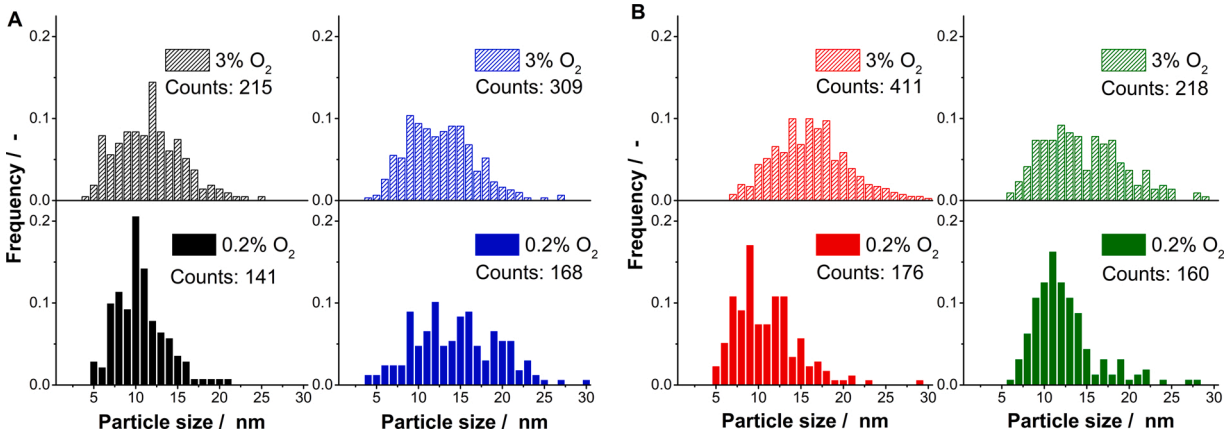

Fig. 3. Observed Ni particle size distributions from STEM-EDX for initial O_2 concentrations of 0.2 % (filled bars) and 3 % (patterned bars). From left to right: 0.04, 0.08 (both A), 0.12 and 0.24 g g^{-1} (both B).

function of time-on-stream during dry reforming over Ni/ Al_2O_3 is shown in Fig. 4. The catalytic activity of the samples increases with Ni loading. Interestingly though, increasing the loading of Ni from 0.08 g g^{-1} to 0.12 g g^{-1} has only a minor effect on the methane conversion. Somewhat faster deactivation at longer runtimes can be noted for the catalyst with 0.08 g g^{-1} Ni loading. For higher Ni loadings the initial deactivation curve is steeper than that for 0.04 g g^{-1}. After the initial period of deactivation however (i.e. after 2–3 h TOS) the different curves can almost be seen as the same curve shifted vertically.

The effect of passivation and reactivation depend substantially on the Ni loading of the catalyst (Fig. 5). For the highest loading of 0.24 g g^{-1} a reduction in conversion can be observed already after a passivation treatment starting with 1 % O_2. Reducing the loading to 0.08 g g^{-1} or 0.12 g g^{-1} leads to no visible impact of the passivation on the conversion. Interestingly, for the lowest loading of 0.04 g g^{-1}, passivation and reactivation lead to an increased conversion, comparable to that of the 0.08 g g^{-1} sample.

STEM-EDX analysis already indicated sintering of Ni particles during passivation for higher Ni loadings and higher initial O_2 concentrations. Consequently, the differences in the catalyst activity can be attributed to the overheating of metal particles during catalyst passivation. If the loading is high enough, such as for 0.24 g g^{-1}, enough heat is generated even on a 25 mg-scale to cause noticeable sintering of Ni particles and thus a reduction of catalytic activity. If the overall amount of Ni is lower, less heat is generated and little or no sintering takes place. The increase in catalytic activity for 0.04 g g^{-1} has a different origin. Here the existence of less reducible Ni species such as $NiAl_2O_4$ needs to be taken into account. [49] While $NiAl_2O_4$ itself is not as easy to reduce as NiO, successive redox cycles have been shown to reduce such Ni species even below the nominal reduction temperature of $NiAl_2O_4$. [50] 0.04 g g^{-1} is the system with the highest dispersion of Ni and consequently the largest Ni—Al_2O_3 interface. This explains a higher percentage of $NiAl_2O_4$ for 0.04 g g^{-1} and a higher impact of a cyclic redox treatment.

The onset of sintering for 0.24 g g^{-1} even with our mildest passivation procedure makes this sample a good starting point for further study. If a mild passivation procedure already causes overheating, a higher initial O_2 concentration should exacerbate local overheating even further. To verify this hypothesis, we performed catalytic experiments on 0.24 g g^{-1} after reduction and passivation with different initial O_2 concentrations. However, when we increased the initial O_2 concentration during the passivation of 0.24 g g^{-1}, we noted no impact on the catalytic activity in the conversion plots. A further drop in activity was only observable, when we increased the overall catalyst amount from 25 mg to 400 mg during reduction and passivation. This was done to increase the local peak temperatures during passivation further due to scale effects.

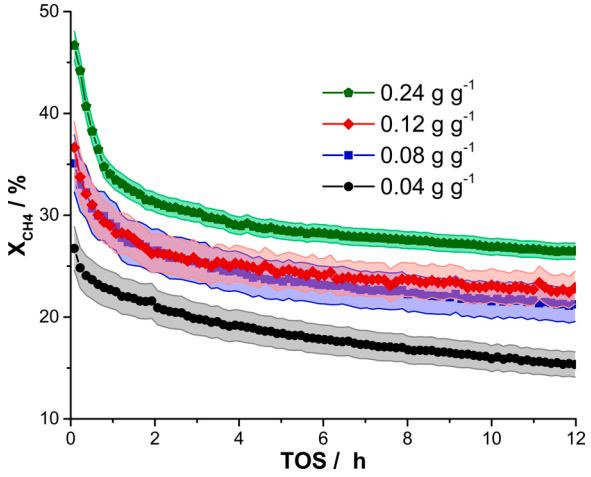

Fig. 4. Methane conversion over TOS for Ni/ Al_2O_3 catalysts pre-reduced in the reactor at 800 °C (Conditions: 10 mg sample, 650 °C, 100 mL min^{-1} (25 % CH_4, 25 % CO_2 in N_2); highlighted areas represent the observed experimental error).

The conversion profiles and the coke contents determined after the respective runs are shown in Figs. 6 and 7 respectively. The coke content after reaction is more sensitive to the exact conditions used during catalyst passivation. Compared to the reference measurement, a sample that underwent mild passivation contains more coke (61 wt.% vs. 52 wt. %). Increasing the initial O_2 concentration during passivation to 3 % increases the coke content even further. Compared to this, a sample directly exposed to air after reduction contains a similar amount of coke (69 vs. 67 wt.%). However, when the overall catalyst amount was scaled to 400 mg, the direct exposure to air led to a significant drop in coke formation.

This result on a 400 mg scale may not be discusses in isolation. If the catalyst is again reduced at 800 °C for 1 h before reaction (instead of heated in H_2 to 650 °C), the catalytic activity is somewhat higher. However, the catalyst deactivation is more pronounced than when passivation is carried out on a smaller scale and after 12 h of reaction the conversion is comparable, regardless of the reduction temperature. At the same time a reduction at higher temperatures means that the coke content once again reaches almost 70 wt.%.

These results fit nicely with the hypothesis of sintering due to the local overheating. If the Ni particles sinter, the larger Ni particles cause more coke formation. The observations for the passivation on a 400 mg scale show that too much heat generation causes additional changes in the catalyst. It seems that then more stable oxidic Ni species are formed that need higher temperatures to reduce. The data on coke formation are not in agreement with the typical observations on $NiAl_2O_4$ catalysts. Different research groups reported highly stable methane reforming catalysts with little coke formation when reducing $NiAl_2O_4$ [19,51]. If $NiAl_2O_4$ formation did take place, it was accompanied by considerable Ni sintering. The reduction of smaller Ni-containing species could not have caused an increase of the coke content by 20 wt.%.

This closer analysis of the sample 0.24 g g^{-1} thus shows the effects that passivation can already have when operating on a scale of 25 mg. The samples with a lower overall Ni loading can be used to elucidate, how quickly overheating during passivation causes Ni sintering. We repeated the variation of the initial O_2 concentration during passivation for the remaining samples. As before, the initial O_2 concentration during passivation does not affect the conversion when passivating 25 mg (Fig. S6). However, a closer analysis of the coke content after reaction provides more insight as can be seen in Fig. 8.

If the loading of Ni is kept sufficiently low (0.04 g g^{-1}), passivation procedures starting at 1 % or 3 % do not lead to an increase in the coke content. If the Ni content is increased to 0.08 g g^{-1}, an initial O_2 concentration of 1 % is still mild enough, while 3 % lead to higher coke contents. For an overall loading of 0.12 g g^{-1} even 1 % of O_2 is too harsh, causing an immediate increase in coking. To put this result into perspective, 25 mg of sample with a Ni loading of 0.12 g g^{-1} is equivalent to a total Ni amount of approx. 2.4 mg. The amount of Ni actually oxidized during passivation will be even smaller. Therefore, it can be said that the existence of overheating during the passivation of Ni/ Al_2O_3 systems is almost independent of scale. This must be taken into account when using passivation and reactivation during catalyst characterization to obtain relevant results.

At the same time, these results highlight the potential of using dry reforming as a model reaction to probe nickel sintering. Through this approach, sintering could already be observed for a loading of 0.08 g g^{-1} and an initial O_2 concentration of 3 %. A STEM-EDX analysis of the same sample did not show any signs of sintering.

4. Conclusions

Four Ni/ Al_2O_3 catalysts with different loadings of Ni were synthesized via incipient wetness impregnation. A high Ni dispersion for all catalysts was confirmed with TPR, BET, TEM and N_2O titration

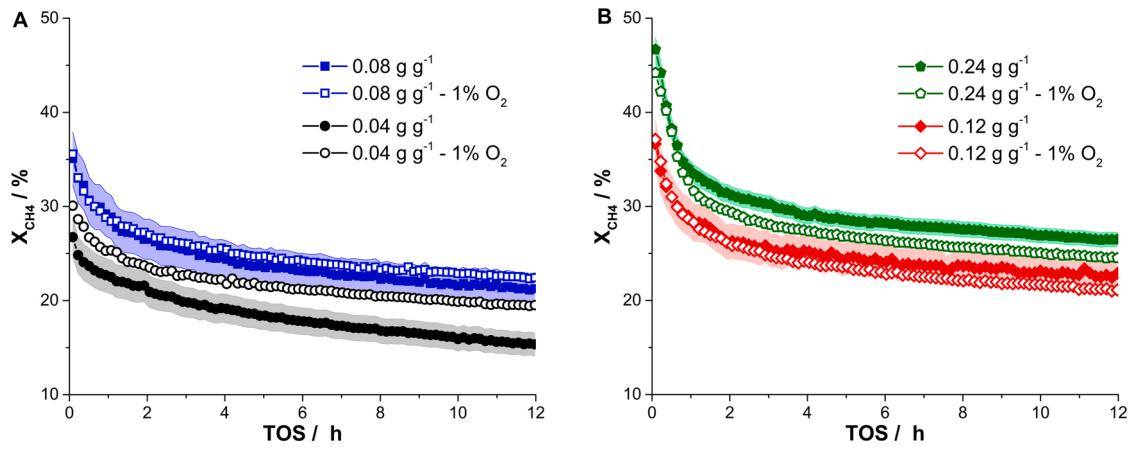

Fig. 5. Methane conversion over TOS for catalysts purely reduced in the reactor (closed symbols) or with previous reduction and passivation starting with 1 % O_2 (half-open symbols), separated for 0.04 and 0.08 g g^1 (A) and 0.12 and 0.24 g g^{-1} (B) (10 mg sample, 650 °C, 100 mL min^{-1} (25 % CH_4, 25 % CO_2 in N_2)).

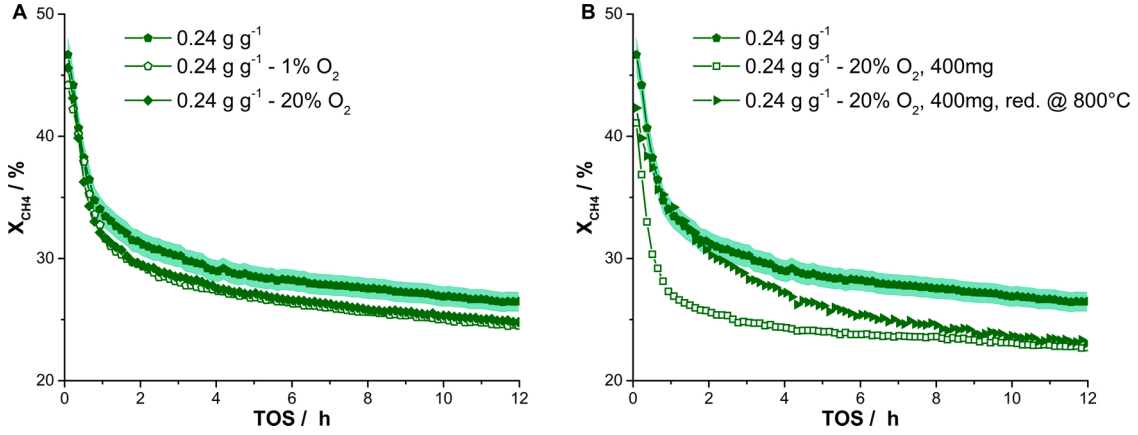

Fig. 6. Impact of the initial O_2 concentration during passivation on a 25 mg scale on methane conversion (A) for 0.24 g g^{-1} and the effect of a 400 mg scale (B) (10 mg sample, 650 °C, 100 mL min^{-1}, 25 % CH_4, 25 % CO_2 in N_2).

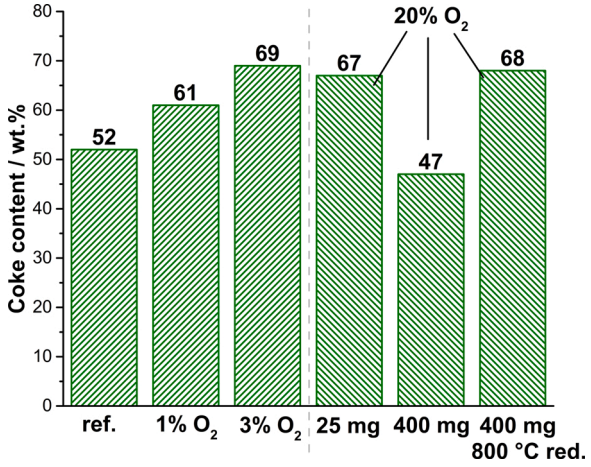

Fig. 7. Impact of the different passivation procedures on the coke content after reaction (10 mg sample, 650 °C, 100 mL min^{-1}, 25 % CH_4, 25 % CO_2 in N_2).

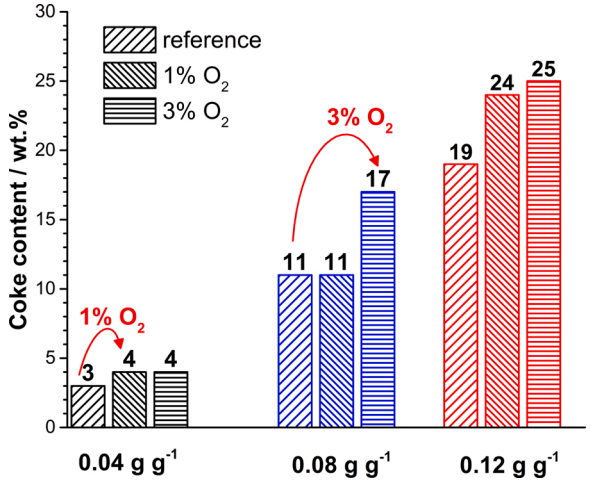

Fig. 8. Coke content after reaction for Ni loadings (up to 0.12 g g^{-1}) and different passivation procedures, 10 mg sample, 650 °C, 100 mL min^{-1} (25 % CH_4, 25 % CO_2 in N_2).

techniques. The impact of catalyst passivation and reactivation on the catalytic properties of the Ni/ Al_2O_3 materials was evaluated in methane dry reforming. Despite the low catalyst amounts used for the experiments, a strong effect of the passivation conditions was observed. We suggest that this is mostly caused by a local overheating during the passivation and consequently sintering of the Ni particles. This in turn enhances the coking for higher Ni loadings and/ or higher initial O_2 concentrations. Importantly, problems during the passivation of Ni/ Al_2O_3 catalysts are almost independent of the catalyst bed volume and can occur even on low-volume lab scale reactors. Only for very low

loadings or sufficiently mild passivation procedures can a constant Ni dispersion be achieved. Thus, even when working on a laboratory scale, an initial O_2 concentration during passivation of lower than 1% is advisable. For catalysts with high Ni loadings or in larger quantities, significantly lower O_2 concentrations may be necessary. Furthermore, this study highlights how dry reforming of methane can be used as a probe reaction to compare the Ni surface area of different samples. The amount of sample necessary is one order of magnitude lower than for classical measurement techniques such as H2 chemisorption.

Declaration of Competing Interest

The authors declare that they have no known competing financial interests or personal relationships that could have appeared to influence the work reported in this paper.

CRediT authorship contribution statement

Robert Franz: Investigation, Conceptualization, Writing - original draft. **Frans D. Tichelaar:** Investigation. **Evgeny A. Uslamin:** Supervision, Writing - review & editing. **Evgeny A. Pidko:** Supervision, Writing - review & editing.

Acknowledgements

Financial support by the CatC1Chem project of NWO, BASF, SABIC and Sasol is gratefully acknowledged. E.A.U. thanks the Tyumen region for partial support within the framework of the grant agreement in the form of a grant to non-profit organizations no. 89-don.

Appendix A. Supplementary data

Supplementary material related to this article can be found, in the online version, at doi:https://doi.org/10.1016/j.apcata.2021.117987.

References

[1] J.R. Rostrup-Nielsen, J. Sehested, J.K. Nørskov, Hydrogen and synthesis gas by steam- and CO2 reforming. Adv. Catal., Academic Press, 2002, pp. 65–139.
[2] M. Akri, S. Zhao, X. Li, K. Zang, A.F. Lee, M.A. Isaacs, W. Xi, Y. Gangarajula, J. Luo, Y. Ren, Y.-T. Cui, L. Li, Y. Su, X. Pan, W. Wen, Y. Pan, K. Wilson, L. Li, B. Qiao, H. Ishii, Y.-F. Liao, A. Wang, X. Wang, T. Zhang, Nat. Comm. 10 (2019) 5181.
[3] J.M. Ginsburg, J. Piña, T. El Solh, H.I. de Lasa, Ind. Eng. Chem. Res. 44 (2005) 4846–4854.
[4] C. Vogt, M. Monai, G.J. Kramer, B.M. Weckhuysen, Nat. Catal. 2 (2019) 188–197.
[5] W.L. Vrijburg, J.W.A. van Helden, A. Parastaev, E. Groeneveld, E.A. Pidko, E.J. M. Hensen, Catal. Sci. Tech. 9 (2019) 5001–5010.
[6] Z. Zhang, T. Wei, G. Chen, C. Li, D. Dong, W. Wu, Q. Liu, X. Hu, Fuel 250 (2019) 176–193.
[7] W.L. Vrijburg, E. Moioli, W. Chen, M. Zhang, B.J.P. Terlingen, B. Zijlstra, I.A. W. Filot, A. Züttel, E.A. Pidko, E.J.M. Hensen, ACS Catal. 9 (2019) 7823–7839.
[8] W.L. Vrijburg, J.W.A. van Helden, A.J.F. van Hoof, H. Friedrich, E. Groeneveld, E. A. Pidko, E.J.M. Hensen, Catal. Sci. Tech. 9 (2019) 2578–2591.
[9] M.J.F.M. Verhaak, A.J. van Dillen, J.W. Geus, Catal. Lett. 26 (1994) 37–53.
[10] Y. Nakagawa, H. Nakazawa, H. Watanabe, K. Tomishige, ChemCatChem 4 (2012) 1791–1797.
[11] E.-J. Shin, M.A. Keane, Ind. Eng. Chem. Res. 39 (2000) 883–892.
[12] J. Xiong, J. Chen, J. Zhang, Catal. Commun. 8 (2007) 345–350.
[13] K. Liu, J. Pritchard, L. Lu, R. van Putten, M.W.G.M. Verhoeven, M. Schmitkamp, X. Huang, L. Lefort, C.J. Kiely, E.J.M. Hensen, E.A. Pidko, Chem. Commun. 53 (2017) 9761–9764.
[14] P. Andreas, N. Fatemeh, R. Dennis, L. Michal, G. Roger, ChemCatChem 3 (2011) 598–606.
[15] C. Vogt, M. Monai, E.B. Sterk, J. Palle, A.E.M. Melcherts, B. Zijlstra, E. Groeneveld, P.H. Berben, J.M. Boereboom, E.J.M. Hensen, F. Meirer, I.A.W. Filot, B. M. Weckhuysen, Nat. Comm. 10 (2019) 5330.
[16] K.Y. Koo, J.H. Lee, U.H. Jung, S.H. Kim, W.L. Yoon, Fuel 153 (2015) 303–309.
[17] K.Y. Koo, H.-S. Roh, Y.T. Seo, D.J. Seo, W.L. Yoon, S.B. Park, Appl. Catal. A Gen. 340 (2008) 183–190.
[18] Z. Mosayebi, M. Rezaei, A.B. Ravandi, N. Hadian, Int. J. Hydrogen Energy 37 (2012) 1236–1242.
[19] J.L. Rogers, M.C. Mangarella, A.D. D'Amico, J.R. Gallagher, M.R. Dutzer, E. Stavitski, J.T. Miller, C. Sievers, ACS Catal. 6 (2016) 5873–5886.
[20] L. Fratalocchi, G. Groppi, C.G. Visconti, L. Lietti, E. Tronconi, Catal. Today 342 (2020) 79–87.
[21] A.L. Imbault, K.J. Smith, Catal. Lett. 146 (2016) 1886–1891.
[22] P. Dufresne, F. Labruyere, US20060154813A1.
[23] H. van Rensburg, US9387463B2.
[24] R. Zennaro, A. Gusso, P. Chaumette, US6096790A.
[25] C.H. Bartholomew, R.J. Farrauto, J. Catal. 45 (1976) 41–53.
[26] A. Gil, A. Diaz, M. Montes, J. Chem. Soc. Faraday Trans. 87 (1991) 791–795.
[27] B.W. Hoffer, A. Dick van Langeveld, J.-P. Janssens, R.L.C. Bonné, C.M. Lok, J. A. Moulijn, J. Catal. 192 (2000) 432–440.
[28] F. Huber, Z. Yu, S. Lögdberg, M. Rønning, D. Chen, H. Venvik, A. Holmen, Catal. Lett. 110 (2006) 211–220.
[29] M. Popowicz, W. Celler, Int. Chem. Eng. 6 (1966), 63-&.
[30] J.T. Richardson, R.J. Dubus, J. Catal. 54 (1978) 207–218.
[31] B. Vos, E. Poels, A. Bliek, J. Catal. 207 (2002) 1–9.
[32] M. Wolf, N. Fischer, M. Claeys, Catal. Today 275 (2016) 135–140.
[33] C. Vogt, E. Groeneveld, G. Kamsma, M. Nachtegaal, L. Lu, C.J. Kiely, P.H. Berben, F. Meirer, B.M. Weckhuysen, Nat. Catal. 1 (2018) 127–134.
[34] A.N. Subbotin, B.S. Gudkov, Z.L. Dykh, V.I. Yakerson, React. Kinet. Catal. Lett. 66 (1999) 97–104.
[35] A.N. Subbotin, B.S. Gudkov, V.I. Yakerson, Russ. Chem. Bull. 49 (2000) 1373–1379.
[36] S. Arora, R. Prasad, RCS Adv. 6 (2016) 108668–108688.
[37] A.G. Linde, Technologies That Do More with Less, 2019 (Accessed Nov. 19, 2019), https://www.linde-engineering.com/en/about-linde-engineering/success-stories/technologies-more-with-less.html.
[38] H. Düdder, K. Kähler, B. Krause, K. Mette, S. Kühl, M. Behrens, V. Scherer, M. Muhler, Catal. Sci. Tech. 4 (2014) 3317–3328.
[39] T. Roussière, Catalytic Reforming of Methane in the Presence of CO2 and H2O at High Pressure, Department of Chemistry, Karlsruhe Institute of Technology, Karlsruhe, 2013.
[40] H.S. Bengaard, J.K. Nørskov, J. Sehested, B.S. Clausen, L.P. Nielsen, A. M. Molenbroek, J.R. Rostrup-Nielsen, J. Catal. 209 (2002) 365–384.
[41] S. Tada, M. Yokoyama, R. Kikuchi, T. Haneda, H. Kameyama, J. Phys. Chem. C 117 (2013) 14652–14658.
[42] A. Peters, F. Nouroozi, D. Richter, M. Lutecki, R. Gläser, ChemCatChem 3 (2011) 598–606.
[43] C. Li, Y.-W. Chen, Thermochim. Acta 256 (1995) 457–465.
[44] B. Mile, D. Stirling, M.A. Zammitt, A. Lovell, M. Webb, J. Mol. Catal. 62 (1990) 179–198.
[45] D.J. Lensveld, J. Gerbrand Mesu, A. Jos van Dillen, K.P. de Jong, Microporous Mesoporous Mater. 44–45 (2001) 401–407.
[46] S. Sun, K. Fujimoto, Y. Zhang, N. Tsubaki, Catal. Commun. 4 (2003) 361–364.
[47] P. Tabib Zadeh Adibi, V.P. Zhdanov, C. Langhammer, H. Grönbeck, J. Phys. Chem. C 119 (2015) 989–996.
[48] Y. Zhang, Y. Liu, G. Yang, S. Sun, N. Tsubaki, Appl. Catal. A 321 (2007) 79–85.
[49] T. Numaguchi, H. Eida, K. Shoji, Int. J. Hydrogen Energy 22 (1997) 1111–1115.
[50] L. Silvester, D. Ipsakis, A. Antzara, E. Heracleous, A.A. Lemonidou, D.B. Bukur, Energy Fuels 30 (2016) 8597–8612.
[51] L. Zhou, L. Li, N. Wei, J. Li, J.-M. Basset, ChemCatChem 7 (2015) 2508–2516.